Basic Res Cardiol 103:232–243 (2008)
DOI 10.1007/s00395-008-0696-1

ORIGINAL CONTRIBUTION

Peter Schott
Abdul R. Asif
Christopher Gräf
Karl Toischer
Gerd Hasenfuss
Harald Kögler

Myocardial adaptation of energy metabolism to elevated preload depends on calcineurin activity

A proteomic approach

Received: 14 November 2007
Returned for 1. Revision: 10 December 2007
1. Revision received: 18 December 2007
Accepted: 8 January 2008
Published online: 15 February 2008

P. Schott and A.R. Asif contributed equally to this work

Electronic supplementary material The online version of this article (doi:10.1007/s00395-008-0696-1) contains supplementary material, which is available to authorized users.

P. Schott, MD · C. Gräf
K. Toischer · G. Hasenfuss · H. Kögler
Dept. of Cardiology and Respiratory Care
Georg-August-University Göttingen
Göttingen, Germany

P. Schott, MD (✉)
Abteilung für Kardiologie und Pneumologie
Georg-August-Universität Göttingen
Robert-Koch-Straße 40
37075 Göttingen, Germany
Tel.: +49-551/392-624
Fax: +49-551/392-600
E-Mail: pschott@gwdg.de

A.R. Asif
Dept. of Clinical Chemistry
Georg-August-University Göttingen
Göttingen, Germany

BRC 696

Abstract Chronic hemodynamic overload on the heart results in pathological myocardial hypertrophy, eventually followed by heart failure. Phosphatase calcineurin is a crucial mediator of this response. Little is known, however, about the role of calcineurin in response to acute alterations in loading conditions of the heart, where it could be mediating beneficial adaptational processes. We therefore analyzed proteome changes following a short-term increase in preload in rabbit myocardium in the absence or presence of the calcineurin inhibitor cyclosporine A. Rabbit right ventricular isolated papillary muscles were cultivated in a muscle chamber system under physiological conditions and remained either completely unloaded or were stretched to a preload of 3 mN/mm^2, while performing isotonic contractions (zero afterload). After 6 h, proteome changes were detected by two-dimensional gel electrophoresis and ESI-MS/MS. We identified 28 proteins that were upregulated by preload compared to the unloaded group (at least 1.75-fold regulation, all $P < 0.05$). Specifically, mechanical load upregulated a variety of enzymes involved in energy metabolism (i.e., aconitase, pyruvate kinase, fructose bisphosphate aldolase, ATP synthase alpha chain, acetyl-CoA acetyltransferase, NADH ubiquinone oxidoreductase, ubiquinol cytochrome c reductase, hydroxyacyl-CoA dehydrogenase). Cyclosporine A treatment (1 μmol/l) abolished the preload-induced upregulation of these proteins. We demonstrate for the first time that an acute increase in the myocardial preload causes upregulation of metabolic enzymes, thereby increasing the capacity of the myocardium to generate ATP production. This short-term adaptation to enhanced mechanical load appears to critically depend on calcineurin phosphatase activity.

Key words proteomics – cardiac metabolism – calcineurin – mechanical load

Abbreviations 2-DE: Two-dimensional gel electrophoresis, CsA: Cyclosporin A, dpi: Dots per inch, DTT: Dithiotreitol, CoA: Coenzyme A, EDTA: Ethylendiaminetetraacetic acid, ESI-MS/MS: Electrospray ionization tandem mass spectrometry, FFR: Force-frequency relationship, h: Hours, IEF: Isoelectric focusing, IPG: Immobilized pH gradient, i.v.: Intravenouse, K-H: Krebs-Henseleit, min.: Minutes, NFAT: Nuclear factor of activated T cells, PAGE: Polyacrylamide gel electrophoresis, pI: Isoelectric point, PMSF: Phenylmethylsulfonyl fluorid, ppm: Parts per million, rpm: Round per minute, SDS: sodium dodecyl sulfate, Tris: Tris(hydroxymethyl) aminomethanol, Vh: Volts × hours

Introduction

Development of cardiac hypertrophy and failure is associated with chamber remodeling as well as with changes of the phenotype at the level of individual myocyte. The concomitant myocardial dysfunction is largely related to disturbed excitation–contraction-coupling processes, which in turn mainly result from altered expression and function of calcium regulatory proteins [13–15, 23, 25, 26, 35]. Additionally, a disturbed energy metabolism with impaired fatty acid oxidation and lower expression of proteins involved in ATP synthesis occurs during myocardial hypertrophy and heart failure [3, 22, 34]. The altered expression of proteins from metabolic pathways may reflect mitochondrial dysfunction as a feature of the transition from compensated myocardial hypertrophy with preserved fatty acid metabolism [9] to impaired energy metabolism in heart failure [27]. The important signaling pathways mediating a hypertrophic phenotype in cardiomyocytes are the activation of G-proteins, phosphoinositide 3-kinase, certain protein kinase C isoforms, mitogen-activated protein kinases, and the calcium-dependent activation of calcineurin [5, 12, 21].

In the heart, preload and afterload are the characteristic biomechanical features and major determinants of physiological and pathological regulations of gene expression. Preload refers to the passive tension (stretch) on the myocardium caused by the blood during the diastolic ventricular filling phase of the cardiac cycle, while afterload is the wall tension actively generated during the systolic phase. Increases of the pre- or afterload, trigger ventricular remodeling, hypertrophy, and heart failure. Nevertheless, little is known about the load dependent activation of signaling pathways and proteome changes.

It is difficult to study the load dependence of gene expression *in vivo*, because load cannot be experimentally modified without concomitant induction of neurohumoral factors [32]. For studying the influence of the changes in preload on the myocardial proteome, we used a recently developed and validated long-term culture system for multicellular myocardial preparations [18, 19]. This allows us to analyze the impact of mechanical preload on the myocardium independent of other stimuli like afterload or neurohumoral stimulation. In this model, we have recently demonstrated that acutely elevated myocardial preload triggers a short-term adaptational response characterized by enhanced expression of the sarcoendoplasmic reticulum Ca^{2+} ATPase (SERCA2) and improved Ca^{2+} homeostasis [20]. This compensatory process critically depended on calcineurin activity. These data contrast the common hypothesis, that calcineurin mainly has a maladaptive role during the development of myocardial hypertrophy. In fact, previously a beneficial effect of the calcineurin cascade has been described after myocardial infarction concerning the left ventricular remodeling in mice [16]. Here, we used the above described model of enhanced preload in combination with a proteomic approach to test the hypothesis that elevated preload causes a compensatory response reflected by the alterations in the myocardial proteome and furthermore investigated, whether or not these changes depend on the activity of calcineurin. To our knowledge, this study represents the first analysis of myocardial proteome changes exclusively due to altered loading conditions under elimination of additional stimuli such as neuroendocrine stimulation. Furthermore, we demonstrate for the first time that preload-dependent modulation of myocardial energy metabolism is mediated by calcineurin.

Materials and methods

Papillary muscle preparation and mechanical loading

The investigation conforms to the *Guide for the Care and Use of Laboratory Animals* (NIH Publication No. 85-23, revised 1996). Female Chinchilla Bastard rabbits (1.5–2 kg, Charles River Laboratories, Kisslegg, Germany) were heparinized and anesthetized with thiopental sodium (50 mg/kg i.v.). Hearts were rapidly excised and retrogradely perfused with modified Krebs-Henseleit (K-H) solution as described [18]. Right ventricular thin papillary muscles were dissected and mounted under completely unloaded conditions in experimental culture chambers (Scientific Instruments, Heidelberg, Germany) between a force transducer and a hook connected to a micrometer drive allowing for length adjustment. The system is equipped with a servomotor with force-feedback function and allows for cultivation of functionally intact multicellular muscle strip preparations for a period of up to 48 h at 37°C with physiological protein turnover maintained [19]. A schematic of the setup is shown in the online supplement. After raising $[Ca^{2+}]$ in a stepwise manner to 1.0 mM, the K-H solution was replaced with tissue culture medium (M-199, Invitrogen, Karlsruhe, Germany) containing 1.25 mM $[Ca^{2+}]$ and supplemented with 20 IU/l human insulin, 0.2% (w/v) bovine serum albumin, 70 μM streptomycin, 100 IU/ml penicillin, and equilibrated with 100% O_2.

Preparations were allowed to stabilize for 1 h under continuous end-to-end electrical stimulation at 1 Hz (amplitude 3–5 V) and then remained either completely unloaded or were stretched progressively over the course of 30 min to a resting tension of 3 mN/mm^2,

corresponding to the length at which isometric tension would be maximum (L_{max}), and allowed to shorten isotonically from this level of resting tension. These loading conditions simulate an isolated increase of preload (preloaded group), while due to the isotonic shortening no afterload is developed. Isotonic shortening was recorded continuously over the entire incubation period of 6 h under the designated loading conditions. In a subset of preparations, the calcineurin/NFAT signaling pathway was blocked by incubating preparations in a medium containing 1 μM of the calcineurin inhibitor, cyclosporin A (CsA, Sigma, Taufkirchen, Germany). CsA was dissolved at 10 mM in ethanol (final concentration 0.01%). The concentration of 1 μM CsA was selected based on a separate set of experiments in which calcineurin activity was assessed. After incubation with CsA, rabbit papillary muscles were lysed in 50 μl calcineurin assay buffer (BioMol, Plymouth Meeting, PA). The Quantizyme Assay System AK-804 was performed according to the manufacturer's procedure using 5 μg of protein homogenates and calcineurin phosphatase activity was measured spectrophotometrically by detecting the free-phosphate released from the calcineurin-specific RII phosphopeptide extracts. In the presence of CsA at the concentration used in our study (1 μM), we found a significant suppression of calcineurin phosphatase activity. A lower CsA concentration that has been previously used in the studies on myocardial calcineurin activity (100 nM) tested in parallel to our hands failed to significantly reduce calcineurin activity (data not shown).

Control preparations were incubated in a medium, supplemented with an equal amount of ethanol but without CsA. At the end of the incubation, muscle preparations were recovered from the culture chamber, rapidly frozen in liquid N_2, and stored at −80°C until later analysis.

For the analysis of the muscle strip contractile function after 6 h of culture with and without CsA, the frequency dependence of force development was assessed by recording muscle shortening at stimulation rates of 1–3 Hz, first immediately after the stretch and again at the end of the 6-h incubation period. At both time points, muscles were stretched to 3.0 mN/mm^2 resting tension and the force development was allowed to reach steady state before the frequency protocol was initiated. Functional data (force–frequency relationship) were analyzed using 2-way ANOVA, with values of $P < 0.05$ considered statistically significant.

Sample preparation for 2-DE

Rabbit papillary muscles were thawed on ice and washed twice in 400 μl ice-cold buffer containing (in mM) TrisBase/HCl pH 7.1 50, KCl 100, EDTA 6, and a mixture of protease inhibitors (in μM) pepstatin A 1, benzamidin 5.8, leupeptin 2.1, PMSF 250 and aprotinin 0.36. After washing, samples were homogenized in 50 μl lysis buffer containing (in mM) TrisBase/HCl pH 7.1 25, KCl 50, EDTA 3, DTT 70, urea 9 M and a mixture of protease inhibitors (in μM) pepstatin A 1, benzamidin 5.8, leupeptin 2.1, PMSF 250, aprotinin 0.36, and 2% (v/v) of ampholytes pH 2–4. After manual homogenization, samples were sonicated for 10 min, followed by 10 min centrifugation at 16,000 rpm. The protein concentrations of the supernatants were measured for samples with a high concentration of urea using the Bio-Rad Protein Assay (Munich, Germany), according to manufacturers' instructions. Samples were stored at −80°C until they were used for 2-DE.

Two-dimensional Gelelectrophoresis (2-DE)

Isoelectric focusing (IEF) was carried out with 18 cm IPG strips (pH 3–10, non-linear gradient, Amersham Biosciences, Freiburg, Germany) in the Protean-IEF cell (Bio-Rad, Munich, Germany) for 32,000 Vh as described before [32]. Protein homogenates were added to the rehydration buffer and analyzed. After focusing, strips were equilibrated in Tris/HCl pH 8.8 50 mM, urea 6 M, glycerol 30 % (v/v), and SDS 2% (w/v) for 10 min in buffer containing 10 mg/ml DTT followed by incubation for 10 min in buffer containing 25 mg/ml iodacetamide. Second dimension electrophoresis was performed using 12% polyacrylamide gels for 30 min at 30 V followed by 250 V for about 5–6 h under continuous cooling to 4°C. The SDS-PAGE was performed in the Protean II XL chamber (Bio-Rad, Munich, Germany) with 200 × 220 × 1 mm gels. Gels were normalized for loading using 150 μg protein homogenates for each gel. Further, spot intensities were normalized for total quantity in the valid spot count mode (PDQuest 7.1 software) and given in ppm.

For estimation of molecular weight and pI of protein spots, we used a 2-DE SDS-PAGE protein standard with a molecular weight ranging from 17.5 to 76 kDa and a pH ranging from 4.5 to 8.5 (Bio-Rad, Munich, Germany). Hence, we were able to divide the gels into six zones with pH ranges from 3 to 4.5, 4.5 to 5.0, 5.0 to 5.4, 5.4 to 6.0, 6.0 to 8.5 and 8.5 to 10.0. Furthermore, we defined five zones of different molecular weights with ranges from 0 to 17.5, 17.5 to 31, 31 to 37, 37 to 66, 66 to 76, and above 76 kDa.

Staining procedures

For the detection of differentially expressed proteins, gels were silver stained according to a protocol modified from Blum et al. [4, 32] as described pre-

viously. Further colloidal coomassie brilliant blue G250 staining (Roth, Karlsruhe, Germany) and Sypro Ruby stain (Invitrogen , Karlsruhe, Germany) in preparative gels for MS/MS analysis were used according to the manufactures manual.

Computer-assisted analysis of 2-DE images

Gel imaging was carried out with a flatbed gel scanning densitometer using a resolution of 300 dpi (Image Scanner, Amersham Biosciences, Freiburg, Germany). PDQuest 7.1 Software (Bio-Rad, Munich, Germany) was used for spot detection, spot quantification, gel matching, and statistical analysis of differences between the experimental groups. The threshold level for differentially expressed proteins was defined as an at least 1.75-fold increase or decrease in spot intensity that was significant at least at the $P < 0.05$ level using a Students *t*-test. The spot intensity was normalized for the total quantity in the valid spot count mode (PDQuest 7.1 software) and is given in ppm.

Identification of 2-DE separated proteins by in-gel digest and ESI-MS/MS

Protein spots excised from silver stained, coomassie blue and Sypro Ruby stained 2-DE were in-gel digested as described before [4, 32]. Extracted peptides were analyzed by ESI-MS/MS analysis for protein identification (details see online supplement). Processed data were searched against MSDB and Swissprot databases using the Mascot search engine (Matrix Science, London, UK; http://www.matrixscience.com), allowing for a peptide mass tolerance of 100 ppm. The search criteria were set to allow one missed cleavage by trypsin, protein modifications were set to methionine oxidation and carbamidomethylation of cysteine. A Protein was accepted as identified if there was a significant Mowse score ($P < 0.05$), correct molecular weight and pI value of the corresponding spot on 2-DE.

Western Immunoblot Analysis

Two-dimensional gel electrophoresis data concerning the protein expression of two proteins (pyruvate kinase and triosephosphate isomerase) were confirmed by western blot analysis.

Rabbit cardiac trabeculae were thawed on ice and chilled in 50 µl homogenization buffer (containing in mmol/L: Na-HEPES 20, pH 7.4, EDTA 2, EGTA 2, DTT 1, phenylmethylsulfonyl fluoride 1,leupeptin 0.05, and iodoacetamide 1). After mechanical homogenization and sonification at 4°C, protein concentrations were determined in triplicate. Samples of 40 µg were denatured in electrophoresis buffer [containing in mmol/l: TRIS/HCl 100, pH 6.8, DTT10, 2% SDS, 2% glycerol, and 0.5% bromophenol blue (wt/vol)] at 95°C and subjected to polyacrylamide gel electrophoresis. Proteins were electroblotted to nitrocellulose membranes, and membranes were blocked overnight at 4°C in 5% (wt/vol) nonfat dry milk in TRIS-buffered saline. Blots were probed with antibodies against glyceraldehyde phophate dehydrogenase (GAPDH; monoclonal, 1:50000, Biotrend Chemikalien, Cologne, Germany), pyruvate kinase (1:2500, polyclonal, Biogenesis, Kingston, USA) and triosephosphate isomerase (1:5000, polyclonal, Novus Biologicals, Kingston, USA). Bands were visualized with enhanced chemiluminescence (Amersham, Freiburg, Germany) and quantified by 2-dimensional scans with a CCD camera system (Multiimager,AlphaInnotech Inc, San Leandro, Calif). GAPDH data were used as the internal standard to control the loaded amount of protein for each sample.

Results

Contractile function of papillary muscles in culture

We assessed the muscle strip contractile function after 6 h of culture with and without 1 µM of the calcineurin inhibitor cyclosporine A. Raising the stimulation rate resulted in a significant frequency-dependent increase in developed twitch tension (positive force-frequency relationship, FFR). A positive FFR is a typical finding in the myocardium exhibiting competent Ca^{2+} homeostasis [6], and demonstrates that under our culture conditions regular muscle function is preserved. In preloaded preparations, the steepness of the frequency-dependent increase in developed twitch tension was significantly higher compared to that of the unloaded preparations ($n = 8$, $P < 0.05$, Fig. 1a). After 6-h incubation in the presence of the calcineurin inhibitor, CsA, muscle strips irrespective of mechanical loading conditions still exhibited a positive FFR. The preload-induced increase in the steepness of the FFR, however, was abolished by CsA treatment (Fig. 1b). Thus, calcineurin activity appears necessary to mediate the preload-induced optimization in Ca^{2+} homeostasis and associated improvement in mechanical performance, indicated by the higher steepness of the FFR.

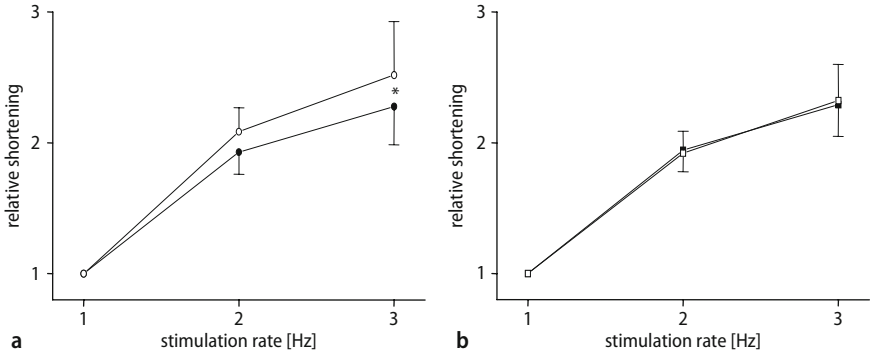

Fig. 1 Preload-dependent change of the force-frequency relationship in untreated (**a**) and CsA-treated (**b**) papillary muscles ($n = 8$ for each group). Force-frequency relationships were recorded at the beginning (*filled symbols*) and the end (*open symbols*) of the 6-hr incubation of stretched muscle strips at optimum preload. Data for each muscle strip are normalized with respect to the force developed at 1-Hz stimulation, * $P < 0.05$

Two-dimensional Gelelectrophoresis

We created two different matchset analyses to detect preload-dependent and calcineurin-mediated alterations of the myocardial proteome. In the first matchset analysis, 2-DE gels of unloaded preparations [unloaded, $n = 6$ (six papillary muscles from six different hearts)] were compared with the preparations subjected to 6 h of increased preload (preloaded, $n = 6$). This matchset enables us to detect the preload-dependent changes of the myocardial proteome. In a second matchset analysis, we compared the unloaded and preloaded papillary muscles after 6 h in culture, in the presence of CsA (1 μM, $n = 6$ each) in the culture medium. CsA leads to specific inhibition of calcineurin activity. Thus, by comparing these two matchsets, we were able to analyze preload-dependent and calcineurin-mediated changes of the myocardial proteome.

A protein was accepted to be differently expressed if there was at least a 1.75-fold difference in the spot intensity associated with a P-value <0.05 (Student's T-test) in all matchsets. Figure 2 shows a representative 2-DE of a papillary muscle, after 6 h of elevated preload in culture. All regulated spots, which where identified by MS/MS analysis in the two matchsets (see above) are labeled with circles.

In the online supplement, a 2-DE with all regulated spots is given (including not identified proteins).

Preload dependent changes of the myocardial proteome

To identify the preload-dependent changes of the myocardial proteome, we compared the 2-DE of the isotonically contracting papillary muscles stretched to L_{max} (preloaded, $n = 6$) with the 2-DE of the preparations remaining completely unloaded ($n = 6$) over 6 h in culture. We identified 28 protein spots with a preload-induced significant change in intensity. All 28 spots were upregulated in the preloaded group compared to that of the unloaded group. Among these 28 proteins, 15 were identified by tryptic in-gel digest and ESI-MS/MS. In Fig. 2, all the identified protein spots are marked and Table 1 lists the identified proteins and their expression levels. In the online supplement, details about MS/MS analysis and statistical comparison of spot intensities are given for each identified protein.

The most prominent finding of this analysis is that a variety of enzymes involved in the energy metabolism were upregulated in myocardium subjected to elevated preload. This applies to the proteins involved in glycolysis [pyruvate kinase, triosephosphate isomerase (2 spots), fructose bisphosphate aldolase A], citric acid cycle (Aconitase), fatty acid beta oxidation and ketone body metabolism (2-hydroxyl-CoA dehydrogenase, acetyl-CoA acetyltransferase), as well as in the respiratory chain [ubicquinol cytochrome C reductase, electron transfer flavoprotein alpha chain, ATP synthase alpha chain (2 spots), NADH-ubiquinone oxidoreductase (2 spots)]. Additionally, the myofilament protein tropomyosin alpha chain and the nuclear protein endonuclease VIII DNA glycosylase were upregulated by increased preload.

The reliability of the level of upregulation determined by 2-DE was confirmed by re-analyzing two arbitrarily selected spots (pyruvate kinase and triosephosphate isomerase) using Western blot analysis. Densitometric analysis confirmed the preload-dependently upregulated protein expression for pyruvate kinase [16,960 ± 241 vs. 24,864 ± 431 arbitrary units (AU), $P < 0.01$, $n = 5$] and triosephosphate isomerase (13,667 ± 1439 vs. 21,614 ± 1,084 AU, $P < 0.01$, $n = 5$). Figure 3 shows 2-DE zoomed gels, Western immunoblot and statistical data for pyruvate kinase (spot 5 in Fig. 2). Corresponding data for the analysis of triosephosphate isomerase are presented in the online supplement.

Some of the significantly regulated proteins (Spots 1, 3, 7 and 8) were present in "spot chains" or at multiple sites on the 2-DE. To elucidate the nature of these protein changes, we performed a screening for possible posttranslational modifications (PTM) on the MS/MS

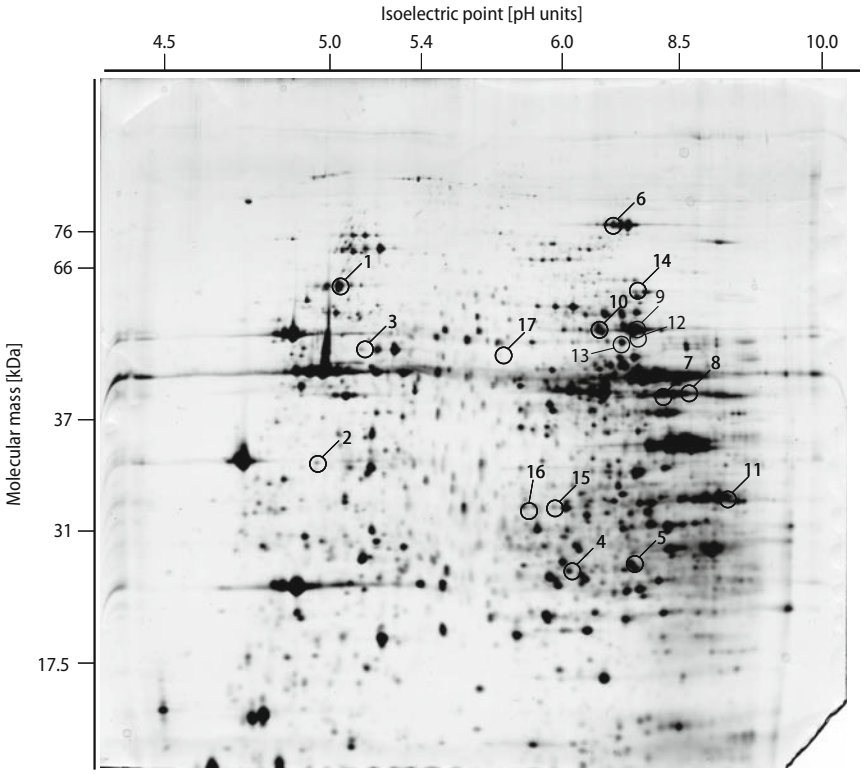

Fig. 2 2-DE of an isotonic papillary muscle after 6 h of culture. First dimension separation employed an IPG strip with a non-linear pH gradient 3–10 (18 cm, Amersham Biosciences) and the second dimension was performed with 12% SDS-PAGE. Total protein load was 150 μg and spots were visualized by silver staining. *Marked spots* indicate identified proteins, which were significantly regulated by comparing the two described matchsets of papillary muscles after 6 h of preload compared to unloaded preparations, and the two CsA groups. *Spot numbers 1–17* correspond to identified proteins and are maintained throughout the tables of the manuscript and online supplement. For details of protein identification and expression changes, see Table 1 and data given in the online supplement

level and used a phosphoprotein stain (Pro-Q-Diamond® = Invitrogen, Karlsruhe, Germany) after 2-DE. However, we were not able to detect PTMs of these proteins (details are given in the online supplement).

Preload dependent changes of the myocardial proteome depend on calcineurin activity

Six hours of elevated preload applied to muscle strips in the presence of the calcineurin inhibitor CsA (unloaded/CsA, $n = 6$; preloaded/CsA, $n = 6$) resulted in the detection of six differently expressed proteins in this matchset. Out of these six proteins, five were down- and only one spot was upregulated. The upregulated spot was identified as heat-shock protein 60 (HSP 60). One of the downregulated proteins was identified by the mass spectrometry as histidine ammonia lyase. To our surprise, only one of the 28 spots found to be upregulated upon analysis of the first matchset (preloaded vs. unloaded without CsA) was significantly altered by mechanical load after inhibition of calcineurin (Spot SSP 4801, see online supplement). However, the change in the protein expression was in the opposite direction: While the protein was significantly upregulated by increased preload with maintained calcineurin signaling (ratio preloaded/unloaded: 2.25, $P = 0.029$), preload caused significant downregulation when calcineurin activity was inhibited (ratio preloaded/CsA/unloaded/CsA: 0.6, $P = 0.046$). Unfortunately, we were unable to identify this spot by MS/MS.

None of the 28 protein spots found to be upregulated by elevated preload was significantly upregulated when a mechanical load was applied after inhibition of calcineurin by CsA. Thus, calcineurin activity is essential to mediate preload-dependent upregulation of these proteins. To illustrate the difference in spot expression under altered loading conditions with and without CsA, Fig. 4 shows zoomed 2-DE for spots 1–3 and the corresponding expression data. Interestingly, HSP 60 (Spot 1), which was upregulated by preload in the preloaded/CsA group, was not upregulated by preload without inhibition of calcineurin.

Importantly, none of the proteins were found to be upregulated by elevated preload but unaltered when preload was applied in the presence of CsA exhibited altered expression levels in unloaded preparations treated with CsA (data not shown). This indicates that CsA indeed specifically affected preload-dependent protein expression changes and did not exert non-specific effects on protein expression, e.g., by affecting mitochondrial membrane permeability.

Table 1 Identified proteins with preload-dependent changes of spot intensity

Spot no.	Identification	Accession no.	Theoretical pI/mass	Observed range of pI/mass	Ratio preloaded/unloaded (*P* value)	Ratio preloadedCysA/ unloadedCysA (*P* values)
1	(CH60_MOUSE) 60 kDa heat shock protein, mitochondrial precursor (Hsp60)	P63038	5.5/61.0	5.0–5.4/37–66	1.21 (ns)	**1.88 (0.03)**
2	(ODPB_HUMAN) Pyruvate dehydrogenase E1 component subunit beta	P11177	5.4/36.8	4.5–5.0/31–37	**3.73 (0.045)**	0.78 (ns)
3	(UQCR1_MOUSE) Ubiquinol-cytochrome-c reductase complex core protein I, mitochondrial precursor	Q9CZ13	5.7/52.7	5.0–5.4/37–66	**3.10 (0.048)**	0.79 (ns)
4	(TPIS_RABIT) Triosephosphate isomerase	P00939	7.0/26.7	6.0–8.5/17.5–31	**5.98 (0.008)**	0.86 (ns)
5	(TPIS_RABIT) Triosephosphate isomerase	P00939	7.0/26.7	6.0–8.5/17.5–31	**3.81 (0.007)**	1.12 (ns)
6	(ACON_PIG) Aconitate hydratase, mitochondrial precursor	P16276	8.2/85.7	6.0–8.5/>76	**7.48 (0.014)**	0.94 (ns)

Spot no.	Identification	Accession no.	Theoretical pI/mass	Observed range of pI/mass	Ratio preloaded/unloaded (*P* value)	Ratio preloadedCysA/ unloadedCysA (*P* value)
7	(ALDOA_RABIT) Fructose-bisphosphate aldolase A (Muscle-type aldolase)	P00883	8.4/39.2	6.0–8.5/37–66	**5.08 (0.006)**	0.85 (ns)
8	(ALDOA_RABIT) Fructose-bisphosphate aldolase A (Muscle-type aldolase)	P00883	8.4/39.2	8.5–10/37–66	**5.04 (0.025)**	0.87 (ns)
9	(ATPA_MOUSE) ATP synthase alpha chain, mitochondrial precursor ATP	Q03265	7.52/56.5	6.0–8.5/37–66	**4.16 (0.007)**	1.12 (ns)
10	(ATPA1_BOVIN) ATP synthase alpha chain heart isoform mitochondrial precursor	P19483	7.52/56.5	6.0–8.5/37–66	**5.98 (0.049)**	0.93 (ns)

Spot no.	Identification	Accession no.	Theoretical pI/mass	Observed range of pI/mass	Ratio preloaded/ unloaded (*P* value)	Ratio preloadedCysA/ unloadedCysA (*P* value)
11	(HCDH_PIG) Short chain 3-hydroxyacyl-CoA dehydrogenase, mitochondrial precursor	P00348	7.6/33.3	8.5–10.0/31–37	**10.0 (0.006)**	1.25 (ns)
12	(NUBM_MOUSE) NADH-ubiquinone oxidoreductase 51 kDa subunit, mitochondrial precursor	Q91YT0	8.4/50.6	6.0–8.5/37–66	**3.21 (0.019)**	1.47 (ns)
13	(NUBM_MOUSE) NADH-ubiquinone oxidoreductase 51 kDa subunit, mitochondrial precursor	Q91YT0	8.4/50.6	6.0–8.5/37–66	**4.41 (0.048)**	1.32 (ns)
14	(KPYK_XENLA) Pyruvate kinase muscle isozyme	Q92122	6.5/57.0	6.0–8.5/37–66	**6.28 (0.014)**	0.88 (ns)
15	(END8_ECO57) Endonuclease VIII	Q8X9C6	8.12/29.6	6.0–8.5/17.5–31	**3.16 (0.009)**	1.22 (ns)

Spot no.	Identification	Accession no.	Theoretical pI/mass	Observed range of pI/mass	Ratio preloaded/ unloaded (*P* value)	Ratio preloadedCysA/ unloadedCysA (*P* value)
16	(ETFA_MOUSE) Electron transfer flavoprotein alpha-subunit, mitochondrial precursor	Q99LC5	5.7/35.0	5.4–6.0/31–37	**2.91 (0.046)**	0.77 (ns)
17	(HUTH_RHIME) histidine ammonia-lyase	O31197	5.7/52.7	5.4–6.0/37–66	0.83 (ns)	**0.27 (0.004)**

Protein identification after tryptic in-gel digest with ESI-MS/MS mass spectrometry and database search. Spot numbers correspond to Figs. 2, 3, 4 of the manuscript and tables of the online supplement. Theoretical molecular mass is in kilo dalton (kDa) and isoelectric point (pI) according to the ExPASY database. Observed mass and pI of identified proteins on 2-DE by using a mass/pI protein standard from 17.5–76 kDa with a pI range from 4.5–8.5 (2-D SDS-PAGE protein standards; Bio-Rad). Ratio preloaded/unloaded and ratio preloadedCysA/unloadedCysA represent the change of spot intensity in these different experimental groups. Significantly changed spot intensities are given in bold letters with the level of statistical significance in parenthesis. For detailed data of spot intensities see the online supplement.

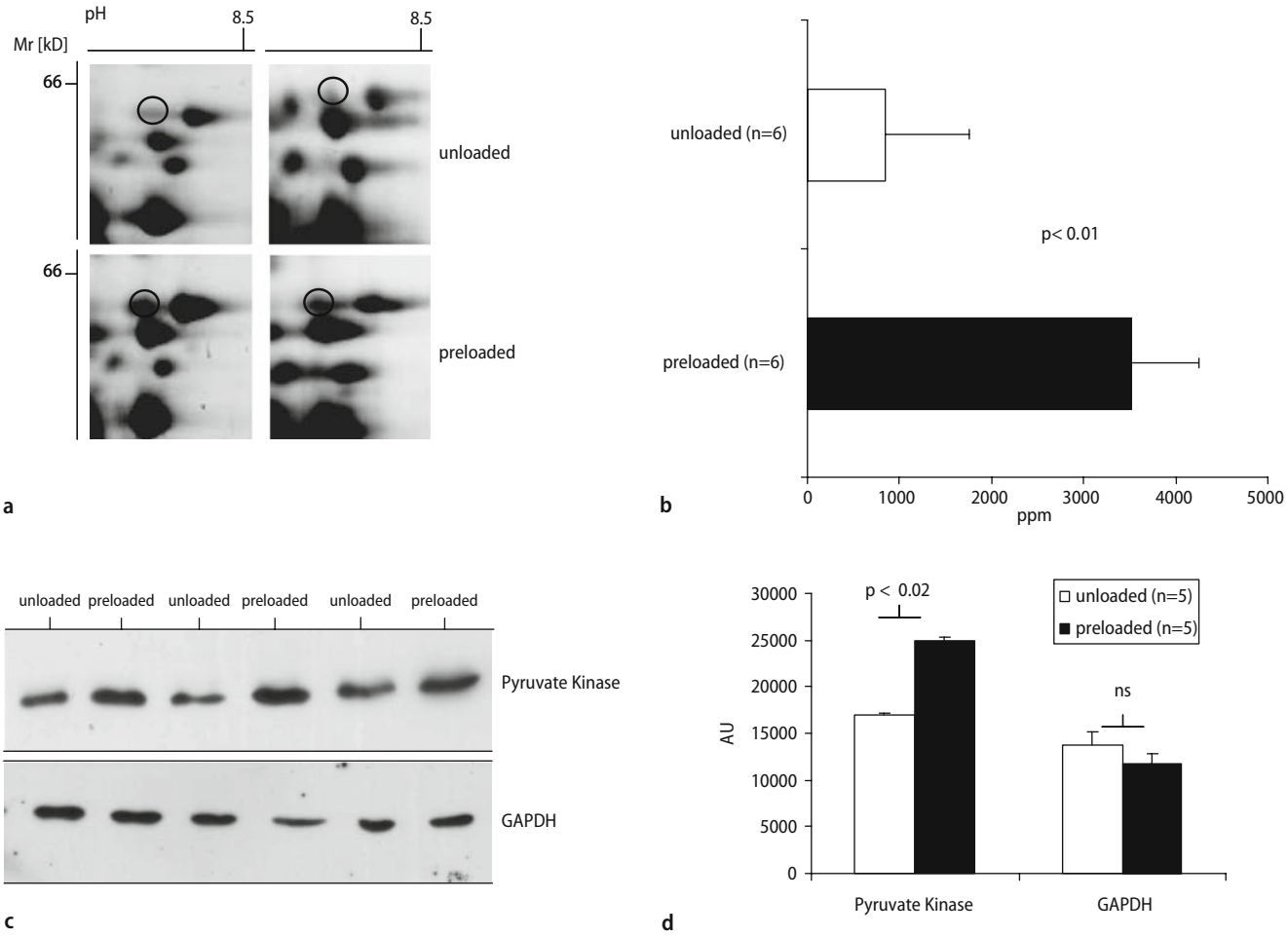

Fig. 3 Expression of pyruvate kinase in unloaded and preloaded preparations. **a** Zoomed 2-DE gels of two unloaded and two preloaded preparations. *Circles* mark spot 5, which was identified as pyruvate kinase by MS/MS analysis. **b** Statistical data concerning spot intensities under unloaded and preloaded conditions of pyruvate kinase in the 2-DE analysis. **c** Western immunoblot for pyruvate kinase and GAPDH, which was used as loading control, under unloaded and preloaded conditions. **d** Statistical data of the Western blot analysis concerning pyruvate kinase and GAPDH expression in unloaded and preloaded preparations. *Mr* molecular weight, *AU* arbitrary units, *ppm* parts per million; data represent mean ± standard deviation

Discussion

We here describe proteome changes caused by 6 h of elevated preload in isolated rabbit myocardium, compared to completely unloaded myocardium. Preload significantly upregulated several proteins of which the majority is involved in various pathways of energy metabolism of the myocardium, including enzymes of glycolysis, citric acid cycle, fatty acid β-oxidation, and mitochondrial respiratory chain. Upon blockade of calcineurin activity with CsA, the observed preload-dependent protein expression changes were completely abolished, while CsA treatment in mechanically unloaded preparations did not affect the expression of proteins found to be regulated by load without CsA. The abundance of metabolic pathways that the upregulated enzymes are derived from indicates that acutely elevated preload triggers a global increase in the capacity of energy metabolism.

The profound suppression of preload-triggered compensatory protein expression changes by calcineurin inhibition is astounding. Calcineurin has been implicated as a key mediator of myocardial hypertrophy under pathological conditions [7, 8, 24], such that calcineurin activation in the myocardium is considered to have deleterious consequences, whereas lower calcineurin activities seem to be cardioprotective [17]. The findings of the present study, however, divert from this hypothesis by suggesting that calcineurin may have a physiological role in the myocardium as a mediator of compensatory short-term adaptation to enhanced biomechanical load, as well. This result is in line with our recent finding that acutely elevated preload caused calcineurin-dependent upregulation of SERCA2 in isolated rabbit myocardium, which was associated with

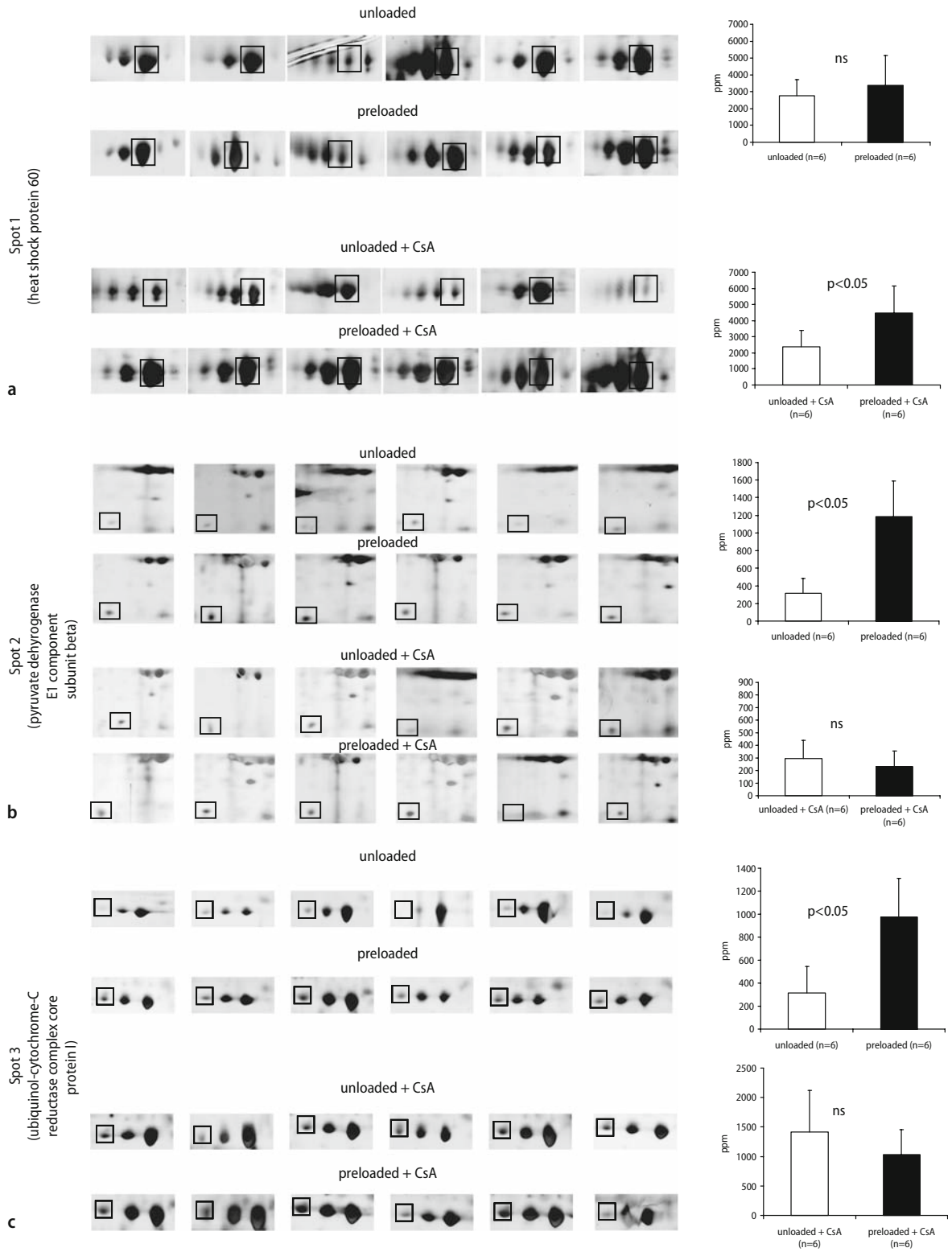

Fig. 4 Illustration of zoomed 2-DE from spots 1–3 and statistical data. **a** Shows zoomed 2-DE of protein spot 1 from each of the gel images for each experimental condition ($n = 6$ for each condition) and statistical data. **b** Shows zoomed gel images and data of protein spot 2 and **c** of protein spot 3. Data are mean ± standard deviation

improved contractility [20]. In this previous publication, we used identical experimental conditions and measured SERCA2a expression by real-time PCR and western blots after 6 h of preload compared to unloaded preparations with and without CsA. A further set of western blot analysis, which confirmed the load-dependent upregulation of SERCA2a expression in unloaded and preloaded muscle preparations is presented in the online supplement.

Acute stretch of myocardium evokes a rapid increase in myofibrillar Ca^{2+} responsiveness followed by an increase in cytosolic [Ca^{2+}], thereby stimulating actin–myosin cross-bridge cycling, and thus force development [2, 36]. This increases the turnover of high-energy phosphate compounds. Upon sustained elevation of load, an adaptation of the energy metabolism would enable the myocardium to cope with this elevated energy demand.

Our assessment of contractile function confirms a significantly enhanced steepness of the frequency-dependent increase in developed twitch tension in preparations preloaded for 6 h, compared to that of unloaded preparations. This load-dependent effect is abolished upon inhibition of calcineurin using CsA. Thus, both the boost in contractility and the upregulation of proteins involved in metabolic pathways by elevated mechanical load occur in a calcineurin-dependent manner. The calcineurin-mediated upregulation of SERCA2 under the same loading conditions that we have recently observed [20] may well account for the improved Ca^{2+}-handling capability of the myocardium that is reflected by the increased steepness of the FFR. SERCA2 is the energetically most efficient mechanism for the diastolic removal of Ca^{2+} from the cytosol, because the pump transports 2 mol of Ca^{2+} ions for each mol of ATP hydrolyzed. This efficiency comes at the price that SERCA is the ATPase with the highest minimal energy requirement in cardiac muscle cells [1, 10]. Since the free energy available from ATP hydrolysis critically depends on the phosphorylation potential, and thus is sensitive to an increase in the concentrations of P_i or ADP, an augmentation of the ATP-generating capacity of the myocytes could facilitate SERCA2 to cope with this energetic burden [37]. This concept is supported by a recent study using computational modeling, which demonstrated that upon an abrupt increase in myocardial energy expenditure concerted activation of glycolysis, mitochondrial dehydrogenases, the electron transport chain, and oxidative phosphorylation serves to keep the concentrations of ATP and ADP constant [38], thereby maintaining the phosphorylation potential at levels required for energy-efficient ATP hydrolysis.

The findings concerning the CsA-dependent expression of metabolic proteins are supported by a recent study using microarray technology and adenovirus-mediated gene transfer of a constitutively active calcineurin mutant into neonatal rat myocytes [31]. The authors demonstrated, that increased calcineurin activity caused upregulation of a variety of enzymes involved in fatty acid metabolism, glycolysis and mitochondrial ATP synthesis. This was associated with the activation of PPARα, which is known to regulate the expression of fatty acid oxidation enzymes, and transcriptional coactivator PGC-1a, which is known to regulate the expression of mitochondrial respiratory chain enzymes.

Changes in the expression of a variety of proteins involved in energy metabolism have been detected in heart failure by performing proteome analysis [3]. It has been suggested that altered expression of proteins from metabolic pathways reflects mitochondrial dysfunction as a feature of the transition from compensated myocardial hypertrophy to heart failure [27]. During the development of mechanical load-induced cardiac hypertrophy, a shift of energy substrate consumption occurs with reduced fatty acid oxidation and increased glucose utilization [28–30]. This has been interpreted as the recapitulation of a fetal gene expression pattern resulting in this substrate switch from fatty acid to glucose and pyruvate utilization [11, 33]. In the present study, the metabolic enzyme expression changes do not indicate that a comparable shift of substrate utilization occurs in our preparations, since the alterations also involve enzymes implicated in fatty acid β-oxidation.

Our findings are made possible by the use of an experimental setting that allows for entirely independent assessment of the effects of various loading conditions and humoral stimuli. This is in contrast to in vivo models of elevated myocardial load, which are, to some extent, obscured by an indispensable accompanying neuroendocrine activation. This is particularly important, since we have previously described an increased expression of enzymes involved in mitochondrial ATP synthesis in neurohumorally stimulated myocardium [32]. The alterations of the myocardial proteome in our study are exclusively induced by elevated preload.

The main limitation of our study is the lack of direct demonstration of calcineurin activation and its abolition by CsA treatment in the loaded and unloaded myocardial preparations. Unfortunately, measurement of calcineurin activity in isolated rabbit papillary muscles is not possible due to technical limitations (for details see the comment in the online supplement).

In conclusion, by using a proteomic approach in combination with an in vitro model of increased myocardial preload, we demonstrate for the first time that elevated preload is associated with upregulation of proteins involved in fatty acid oxidation, glucose

metabolism, and mitochondrial ATP synthesis. These proteome changes seem to be critically linked to a load-dependent calcineurin activity and suggest a physiological role for calcineurin as a mediator of compensatory short-term adaptation to acutely enhanced preload.

Acknowledgments This study was supported by the German Research Foundation (DFG, SFB/TR2 and grant KO 1873/2-1) and the German National Genome Research Network (NGFN).

References

1. Alonso GL, Gonzalez DA, Takara D, Ostuni MA, Sanchez GA (2001) Kinetic analysis of a model of the sarcoplasmic reticulum Ca-ATPase, with variable stoichiometry, which enhances the amount and the rate of Ca transport. J Theor Biol 208:251–260
2. Alvarez BV, Perez NG, Ennis IL, Camilion de Hurtado MC, Cingolani HE (1999) Mechanisms underlying the increase in force and Ca(2+) transient that follow stretch of cardiac muscle: a possible explanation of the Anrep effect. Circ Res 85:716–722
3. Arrell DK, Neverova I, Van Eyk JE (2001) Cardiovascular proteomics: evolution and potential. Circ Res 88:763–773
4. Blum H, Beier H, Gross HJ (1987) Improved silver staining of plant proteins, RNA and DNA in polyacrylamide gels. Electrophoresis 8:93–99
5. Chen QM, Tu VC, Purdon S, Wood J, Dilley T (2001) Molecular mechanisms of cardiac hypertrophy induced by toxicants. Cardiovasc Toxicol 1:267–283
6. Crozatier B (1998) Force-frequency relations in nonfailing and failing animal myocardium. Basic Res Cardiol 93(Suppl 1):46–50
7. De Windt LJ, Lim HW, Bueno OF, Liang Q, Delling U, Braz JC, Glascock BJ, Kimball TF, del Monte F, Hajjar RJ, Molkentin JD (2001) Targeted inhibition of calcineurin attenuates cardiac hypertrophy in vivo. Proc Natl Acad Sci USA 98:3322–3327
8. De Windt LJ, Lim HW, Taigen T, Wencker D, Condorelli G, Dorn GW 2nd, Kitsis RN, Molkentin JD (2000) Calcineurin-mediated hypertrophy protects cardiomyocytes from apoptosis in vitro and in vivo: an apoptosis-independent model of dilated heart failure. Circ Res 86:255–263
9. Degens H, de Brouwer KF, Gilde AJ, Lindhout M, Willemsen PH, Janssen BJ, van der Vusse GJ, van Bilsen M (2006) Cardiac fatty acid metabolism is preserved in the compensated hypertrophic rat heart. Basic Res Cardiol 101:17–26
10. Ebus JP, Stienen GJ (1996) Origin of concurrent ATPase activities in skinned cardiac trabeculae from rat. J Physiol 492(Pt 3):675–687
11. Feldman AM, Weinberg EO, Ray PE, Lorell BH (1993) Selective changes in cardiac gene expression during compensated hypertrophy and the transition to cardiac decompensation in rats with chronic aortic banding. Circ Res 73:184–192
12. Grammer JB, Bleiziffer S, Monticelli F, Lange R, Bauernschmitt R (2006) Calcineurin and matrix protein expression in cardiac hypertrophy: evidence for calcineurin B to control excessive hypertrophic signaling. Basic Res Cardiol 101:292–300
13. Hasenfuss G, Mulieri LA, Leavitt BJ, Allen PD, Haeberle JR, Alpert NR (1992) Alteration of contractile function and excitation-contraction coupling in dilated cardiomyopathy. Circ Res 70:1225–1232
14. Hasenfuss G, Pieske B (2002) Calcium cycling in congestive heart failure. J Mol Cell Cardiol 34:951–969
15. Hasenfuss G, Reinecke H, Studer R, Meyer M, Pieske B, Holtz J, Holubarsch C, Posival H, Just H, Drexler H (1994) Relation between myocardial function and expression of sarcoplasmic reticulum Ca(2+)-ATPase in failing and nonfailing human myocardium. Circ Res 75:434–442
16. Heineke J, Ruetten H, Willenbockel C, Gross SC, Naguib M, Schaefer A, Kempf T, Hilfiker-Kleiner D, Caroni P, Kraft T, Kaiser RA, Molkentin JD, Drexler H, Wollert KC (2005) Attenuation of cardiac remodeling after myocardial infarction by muscle LIM protein-calcineurin signaling at the sarcomeric Z-disc. Proc Natl Acad Sci USA 102:1655–1660
17. Ikeda Y, Miura T, Sakamoto J, Miki T, Tanno M, Kobayashi H, Ohori K, Takahashi A, Shimamoto K (2006) Activation of ERK and suppression of calcineurin are interacting mechanisms of cardioprotection afforded by delta-opioid receptor activation. Basic Res Cardiol 101:418–426
18. Janssen PM, Hasenfuss G, Zeitz O, Lehnart SE, Prestle J, Darmer D, Holtz J, Schumann H (2002) Load-dependent induction of apoptosis in multicellular myocardial preparations. Am J Physiol Heart Circ Physiol 282:H349–H356
19. Janssen PM, Lehnart SE, Prestle J, Hasenfuss G (1999) Preservation of contractile characteristics of human myocardium in multi-day cell culture. J Mol Cell Cardiol 31:1419–1427
20. Kögler H, Schott P, Toischer K, Milting H, van Nguyen P, Kassner A, Domeier E, Junge J, Teucher N, Zeitz O, Seilder T, El-Banayosy A, Körfer R, Hasenfuss G (2006) Relevance of brain natriuretic peptide in load-dependent regulation of cardiac sarcoplasmic reticulum Ca^{2+} ATPase expression. Circulation 113:2724–2732
21. Lim HW, De Windt LJ, Steinberg L, Taigen T, Witt SA, Kimball TR, Molkentin JD (2000) Calcineurin expression, activation, and function in cardiac pressure-overload hypertrophy. Circulation 101:2431–2437
22. Maack C, O'Rourke B (2007) Excitation-contraction coupling and mitochondrial energetics. Basic Res Cardiol 102:369–392
23. Meyer M, Schillinger W, Pieske B, Holubarsch C, Heilmann C, Posival H, Kuwajima G, Mikoshiba K, Just H, Hasenfuss G et al. (1995) Alterations of sarcoplasmic reticulum proteins in failing human dilated cardiomyopathy. Circulation 92:778–784
24. Molkentin JD, Lu JR, Antos CL, Markham B, Richardson J, Robbins J, Grant SR, Olson EN (1998) A calcineurin-dependent transcriptional pathway for cardiac hypertrophy. Cell 93:215–228
25. Morgan JP (1991) Abnormal intracellular modulation of calcium as a major cause of cardiac contractile dysfunction. N Engl J Med 325:625–632
26. Pieske B, Kretschmann B, Meyer M, Holubarsch C, Weirich J, Posival H, Minami K, Just H, Hasenfuss G (1995) Alterations in intracellular calcium handling associated with the inverse force-frequency relation in human dilated cardiomyopathy. Circulation 92:1169–1178

27. Razeghi P, Young ME, Alcorn JL, Moravec CS, Frazier OH, Taegtmeyer H (2001) Metabolic gene expression in fetal and failing human heart. Circulation 104:2923–2931
28. Recchia FA, McConnell PI, Bernstein RD, Vogel TR, Xu X, Hintze TH (1998) Reduced nitric oxide production and altered myocardial metabolism during the decompensation of pacing-induced heart failure in the conscious dog. Circ Res 83:969–979
29. Sack MN, Kelly DP (1998) The energy substrate switch during development of heart failure: gene regulatory mechanisms (review). Int J Mol Med 1:17–24
30. Sack MN, Rader TA, Park S, Bastin J, McCune SA, Kelly DP (1996) Fatty acid oxidation enzyme gene expression is downregulated in the failing heart. Circulation 94:2837–2842
31. Schaeffer PJ, Wende AR, Magee CJ, Neilson JR, Leone TC, Chen F, Kelly DP (2004) Calcineurin and calcium/calmodulin-dependent protein kinase activate distinct metabolic gene regulatory programs in cardiac muscle. J Biol Chem 279:39593–39603
32. Schott P, Singer SS, Kogler H, Neddermeier D, Leineweber K, Brodde OE, Regitz-Zagrosek V, Schmidt B, Dihazi H, Hasenfuss G (2005) Pressure overload and neurohumoral activation differentially affect the myocardial proteome. Proteomics 5:1372–1381
33. Schwartz K, Boheler KR, de la Bastie D, Lompre AM, Mercadier JJ (1992) Switches in cardiac muscle gene expression as a result of pressure and volume overload. Am J Physiol 262:R364–R369
34. Tokoro T, Ito H, Suzuki T (1996) Alterations in mitochondrial DNA and enzyme activities in hypertrophied myocardium of stroke-prone SHRS. Clin Exp Hypertens 18:595–606
35. Vahl CF, Bonz A, Timek T, Hagl S (1994) Intracellular calcium transient of working human myocardium of seven patients transplanted for congestive heart failure. Circ Res 74:952–958
36. von Lewinski D, Stumme B, Fialka F, Luers C, Pieske B (2004) Functional relevance of the stretch-dependent slow force response in failing human myocardium. Circ Res 94:1392–1398
37. Xiang JZ, Kentish JC (1995) Effects of inorganic phosphate and ADP on calcium handling by the sarcoplasmic reticulum in rat skinned cardiac muscles. Cardiovasc Res 29:391–400
38. Zhou L, Cabrera ME, Okere IC, Sharma N, Stanley WC (2006) Regulation of myocardial substrate metabolism during increased energy expenditure: insights from computational studies. Am J Physiol Heart Circ Physiol 291:H1036–H1046